Predictions for F2 and FL in e+p

Javier L. Albacete
IPhT-CEA-Saclay

3rd CERN-ECFA-NuPECC Workshop on the LHeC
Chavannes-des-Bogis, 12-13 November 2010

Goal: To compare different theoretical predictions for F2 and FL in e+p scattering for LHeC kinematics based on:

I) Linear QCD evolution: DGLAP and combined DGLAP/BFKL

II) Non-linear QCD evolution: CGC and other saturation approaches

Analyses of HERA data do not provide a clear separation between these two QCD regimes. All the models presented here provide a good description of HERA data

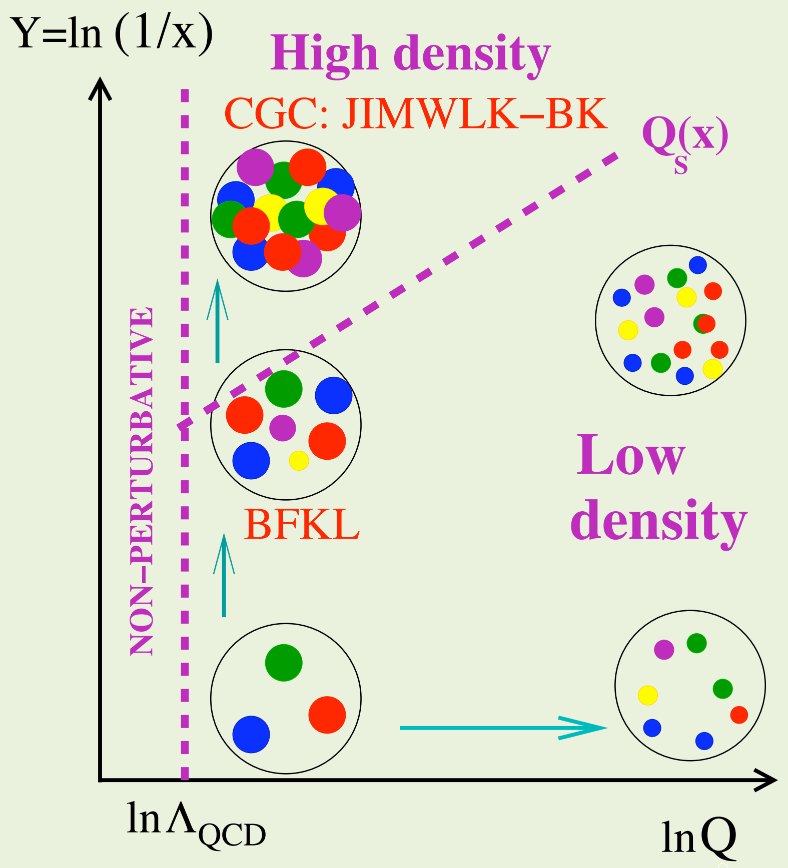

One of the potential goals (duties) of the LHeC is to turn the sketch above into a more quantitative picture.

$\Rightarrow$ Linear QCD evolution

I) DGLAP analysis (NNPDF collaboration. Thanks to J. Rojo)

- NLO DGLAP analysis.
- Neural network approach to avoid bias in the choice of initial conditions
- DGLAP has no predictive power towards small-x: Large uncertainties at small-x:

$$xg(x, Q_0^2) \approx x^{\lambda}(1-x)^{\beta} \ldots \quad \begin{cases} \lambda > 0 & \text{growing gluon} \\ \lambda < 0 & \text{decreasing gluon} \end{cases}$$

II) BFKL/DGLAP analysis (KMS approach. Results by Stasto and Golec-Biernat)

- Small-x BFKL dynamics + kinematic constraints + DGLAP corrections

⇒ Non-linear QCD evolution and other saturation approaches

- The dipole model of DIS is the starting point for (most of) saturation studies in DIS

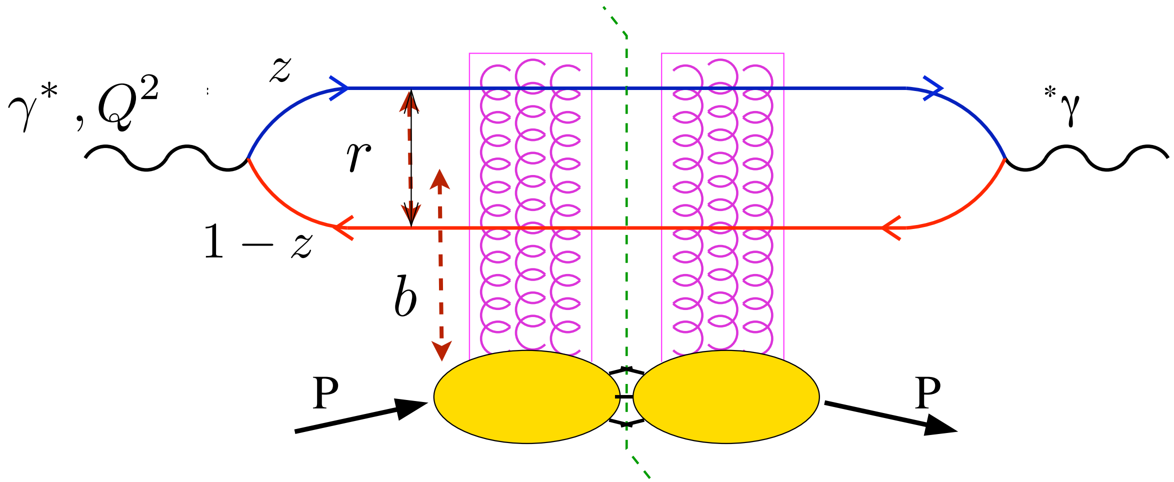

$$\sigma_{T,L}^{\gamma^* P}(x,Q^2) = \sum_{flavors} \int_0^1 dz \int d^2\mathbf{r} \left| \Psi_{T,L}^{\gamma^* \to q\bar{q}}(z,Q,r,m_f) \right|^2 \sigma^{dip}(\tilde{x},r)$$

Photon wavefunction
Calculable within QED

Dipole cross section.
Strong interactions and
x-dependence are here

Different dynamical input in different approaches

(A) classification of dipole models in the market

⇒ According to the physical mechanism driving saturation, i.e (x,Q^2,r)-dynamics:

- Multiple scatterings + DGLAP evolution
- Color Glass Condensate: BK or BFKL+saturation
- Phenomenological models: Regge Theory; non-perturbative input.

⇒ According to their impact parameter dependence

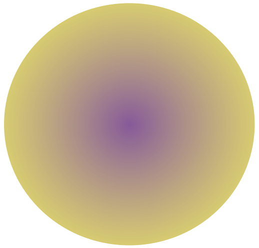

- Homogeneous in the transverse plane
- Some other non-trivial profile (gaussian)

⇒ According to phenomenological details: quark masses, inclusion of charm or beauty contributions, inclusion of kinematic constraints, focus on specific kinematic region ...

⇒ Multiple scatterings + DGLAP evolution: Saturation results from eikonalization of two-gluon exchange: BGBK (Bartels-Golec-Biernat-Kowalski); IPSat (Kowalski-Teaney):

Leading-twist

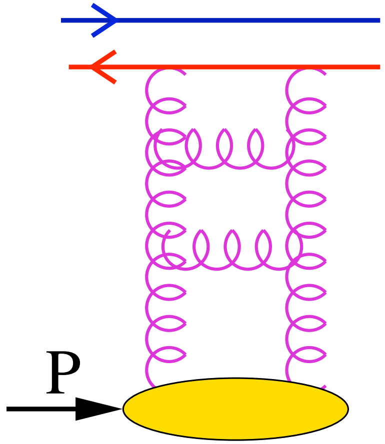

Glauber-Mueller independent rescatterings

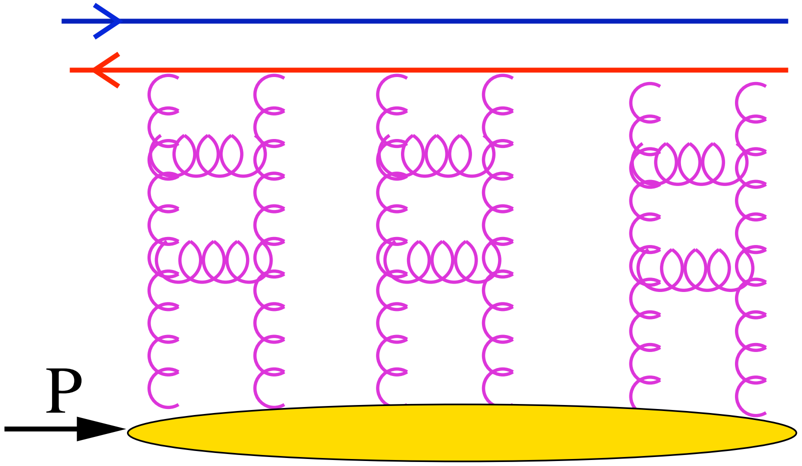

$$\frac{d\sigma^{dip}}{d^2b} \sim \frac{\pi^2}{2\,N_c}\, r^2\, xg(x,Q^2) T_p(b)$$

$$\frac{d\sigma^{dip}}{d^2b} = 1 - \exp\left[-\frac{\pi^2}{2\,N_c}\, r^2\, xg(x,Q^2) T_p(b)\right]$$

Leading $\ln Q^2$ terms in each cascade resummed through DGLAP

All the Bjorken-x dependence is encoded in that of the gluon distribution.

BGBK: Trivial impact parameter dependence: $T_p(b) \sim Q_0^2\, \theta(b_p - b)$

IPSat: Gaussian profile $T_p(b) \sim \exp\left(-b^2/2\,B\right)/(2\pi\, B)$

⇒ Color-Glass-Condensate: Running coupling BK equation

$$\frac{\partial \mathcal{N}(r,x)}{\partial \ln(x_0/x)} = \int d^2 r_1 \, \underbrace{K(r,r_1,r_2)\, [\mathcal{N}(r_1,x) + \mathcal{N}(r_2,x) - \mathcal{N}(r,x)}_{\text{Linear BFKL dynamics}} - \underbrace{\mathcal{N}(r_1,x)\mathcal{N}(r_2,x)]}_{\substack{\text{Non-linear terms} \\ \textit{gluon recombination}}}$$

$$\sigma^{dip}(r,x) = 2\int d^2 b \, \mathcal{N}(r,b,x)$$

- Resums soft gluon emission, including running coupling corrections, to all orders. It also includes non-linear, gluon recombination, terms

- Global fits to inclusive structure functions in e+p coll. yield a good description of data (JLA, Armesto, Milhano, Salgado and Quiroga)

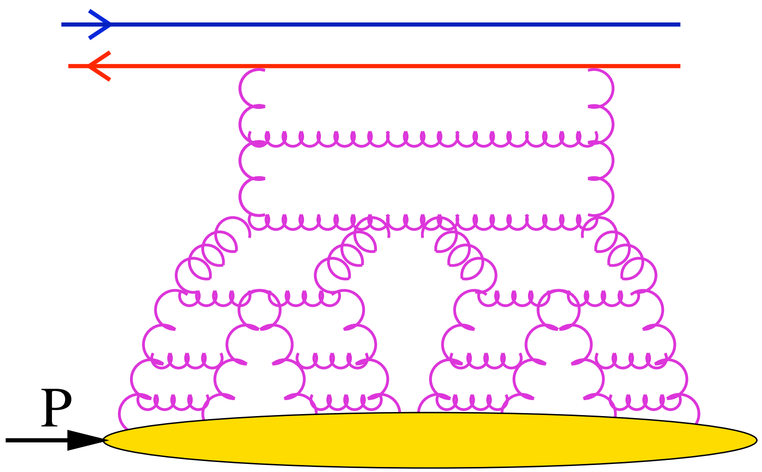

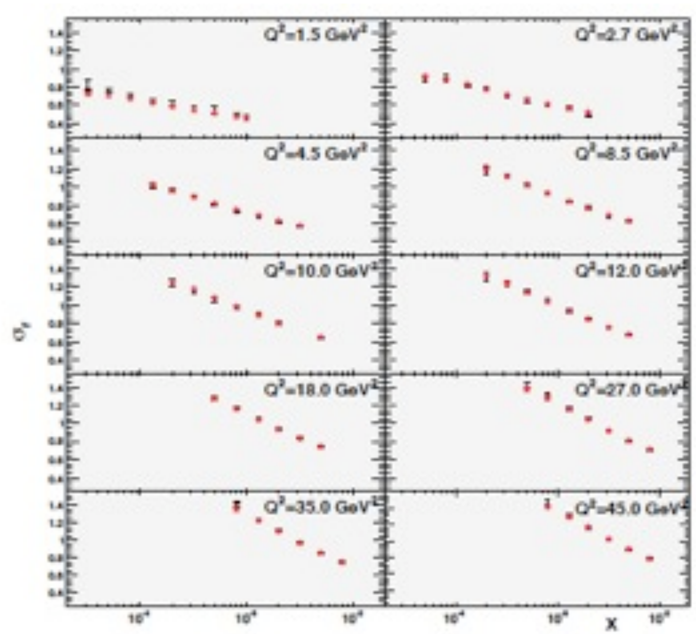

⇒ Color-Glass-Condensate: rcBK equation + other approaches

$$\frac{\partial \mathcal{N}(r,x)}{\partial \ln(x_0/x)} = \int d^2 r_1 \, K(r,r_1,r_2) \, [\mathcal{N}(r_1,x) + \mathcal{N}(r_2,x) - \mathcal{N}(r,x) - \mathcal{N}(r_1,x)\mathcal{N}(r_2,x)]$$

A) Calculations based on numerical solutions of BK eqn with running coupling
JLA-Armesto-Milhano-Salgado (AAMS), Kuokkanan-Rummukainen-Weigert (KRW).

- Trivial impact parameter dependence. Overall normalization fitted to data
- Input: Initial conditions for the evolution, $\mathcal{N}(r,x_0)$. $x_0 \sim 10^{-2}$ (GBW, MV, scaling)
- KRW: Energy conservation (i.e., large-x) effects implemented through

$$K \longrightarrow \left(1 - \frac{\partial}{\partial \ln(x_0/x)}\right) K$$

B) Models based on analytical solutions of BFKL+ absorptive barrier
Iancu-Itakura-Munier-Soyez (CGC), Kowalski-Motyka-Watt (b-CGC)

- Evolution speed λ fitted to data
- b-CGC: Impact parameter dependence.

Bad χ /d.o.f ~ 1.6. Lowest evolution speed of all models: λ ~ 0.16

C) Hybrid BK (large-r)+DGLAP (small-r) + gaussian impact parameter approach
Gotsman-Levin-Lublinsky-Maor

⇒ Phenomenological models

- Golec-Biernat-Wusthoff

$$\begin{cases} \mathcal{N}^{GBW}(x,r) = \theta(R_p - b)\left(1 - \exp\left[-\frac{r^2\,Q_s^2(x)}{4}\right]\right) \\ Q_s^2(x) = Q_0^2\left(\frac{x_0}{x}\right)^{\lambda} \end{cases}$$

- Models based on Regge Theory (+DGLAP evolution)

Forshaw-Shaw FS04: $$\sigma^{dip}(r,x) = \begin{cases} A^{soft}\,x^{-\lambda_{soft}}\,, & \text{for } r > r_1 \quad (\lambda_{soft} \sim 0.66) \\ A^{hard}\,r^2\,x^{-\lambda_{hard}}\,, & \text{for } r < r_0 \quad (\lambda_{hard}\ 0.34) \end{cases}$$

Armesto-Kaidalov-Salgado-Tywoniuk:
- Regge model including unitarity effects for $Q^2<Q_0^2$
- DGLAP evolution for $Q^2>Q_0^2$

- "Strong coupling" dipole from AdS/CFT (Valid for $Q^2 < 2$ GeV^2) Kovchegov-Lu-Rezaeian
- Models tuned to fit also RHIC data.
- Others (my apologies).

Extrapolation for F2 in the LHeC kinematic regime:

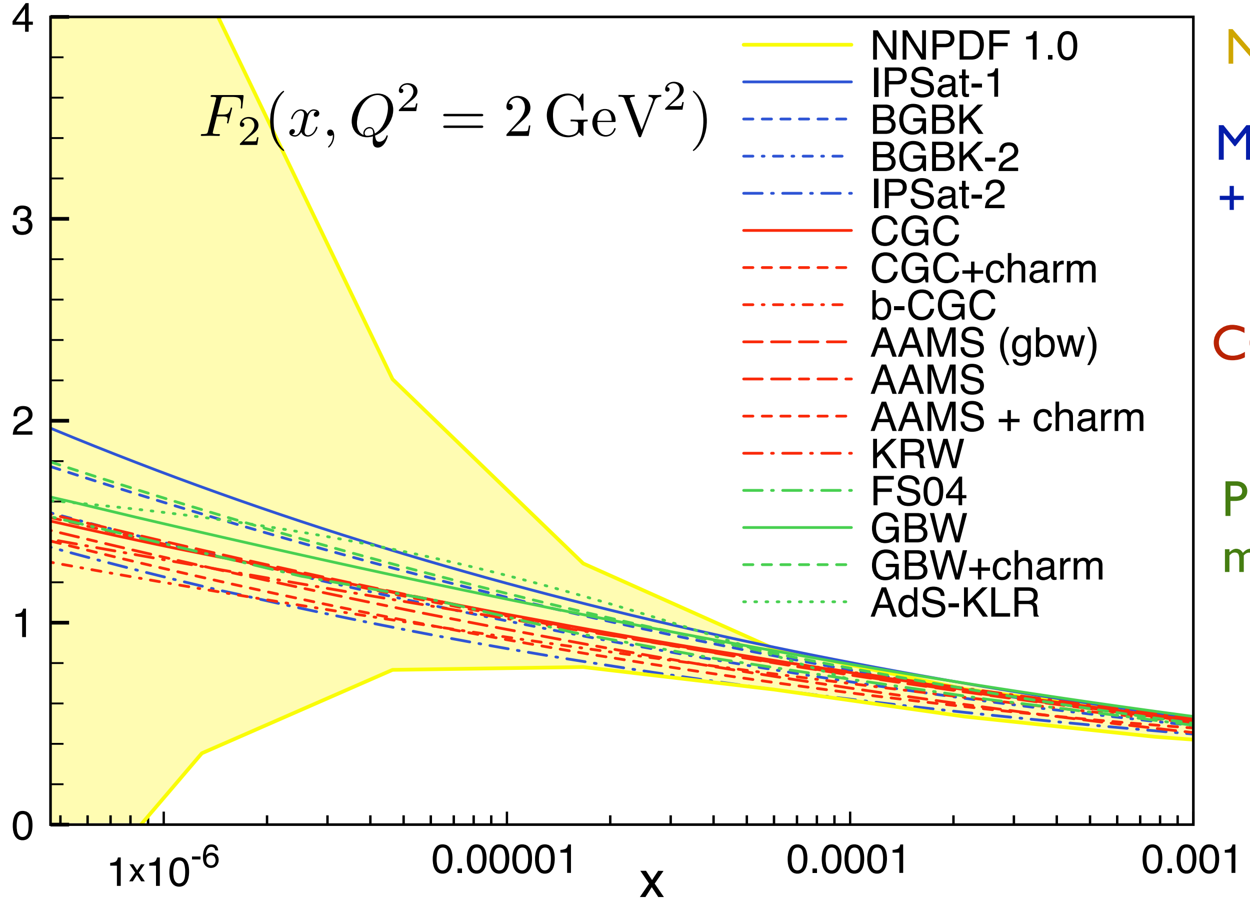

NNPDF DGLAP

Multiple scatterings +DGLAP evolution

CGC-saturation

Phenomenological models

Remarks:

- DGLAP uncertainty band blows at small-x
- Small spread among various non-linear/saturation models

Extrapolation for FL in the LHeC kinematic regime:

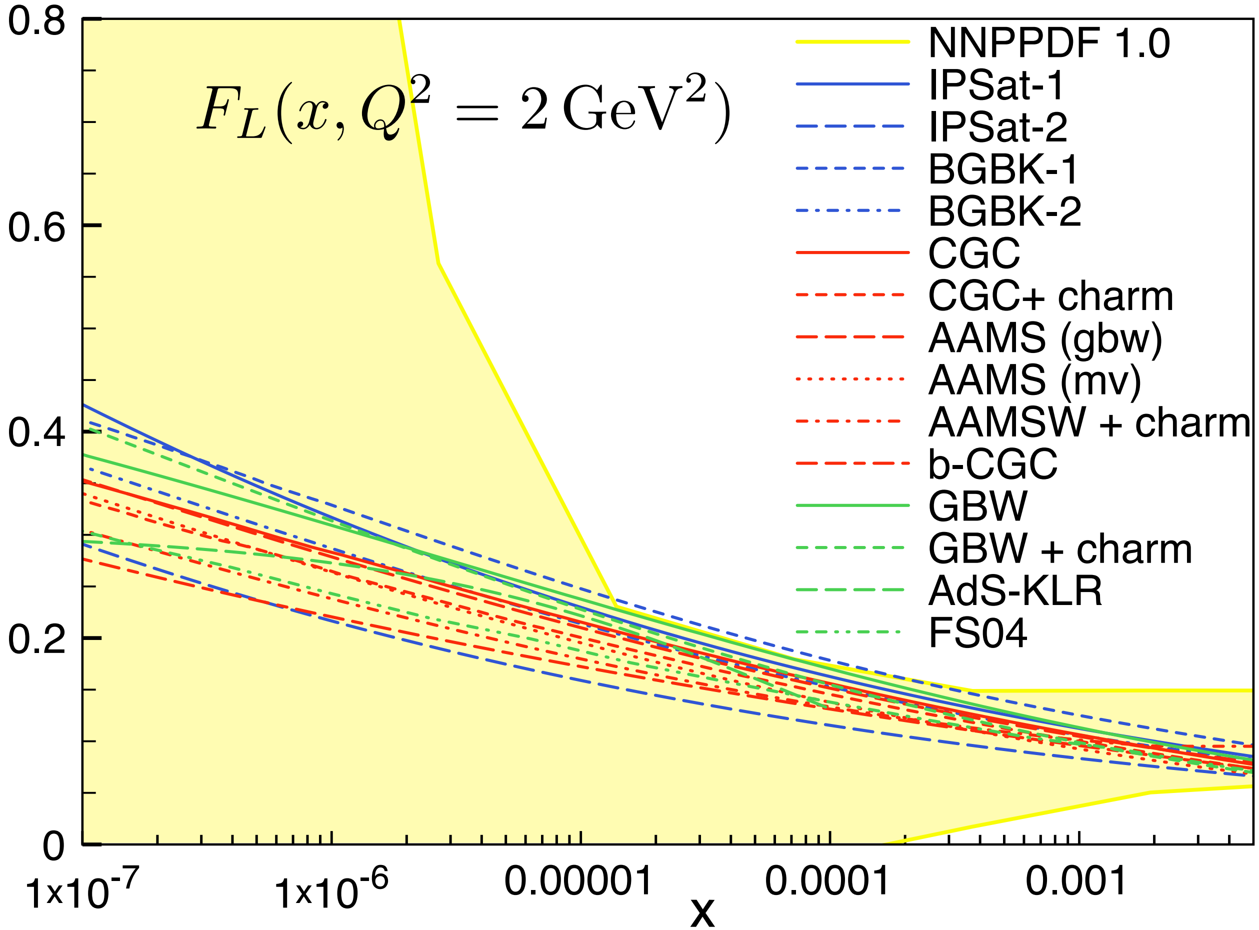

NNPDF DGLAP

Multiple scatterings +DGLAP evolution

CGC-saturation

Phenomenological models

Remarks:

- DGLAP uncertainty band blows at small-x
- Small spread among various non-linear/saturation models

Filtering:

- Consider only models with a clear QCD input
- Perform calculations at a higher Q^2=10 GeV^2
- Include pseudodata

Extrapolation for F2 in the LHeC kinematic regime:

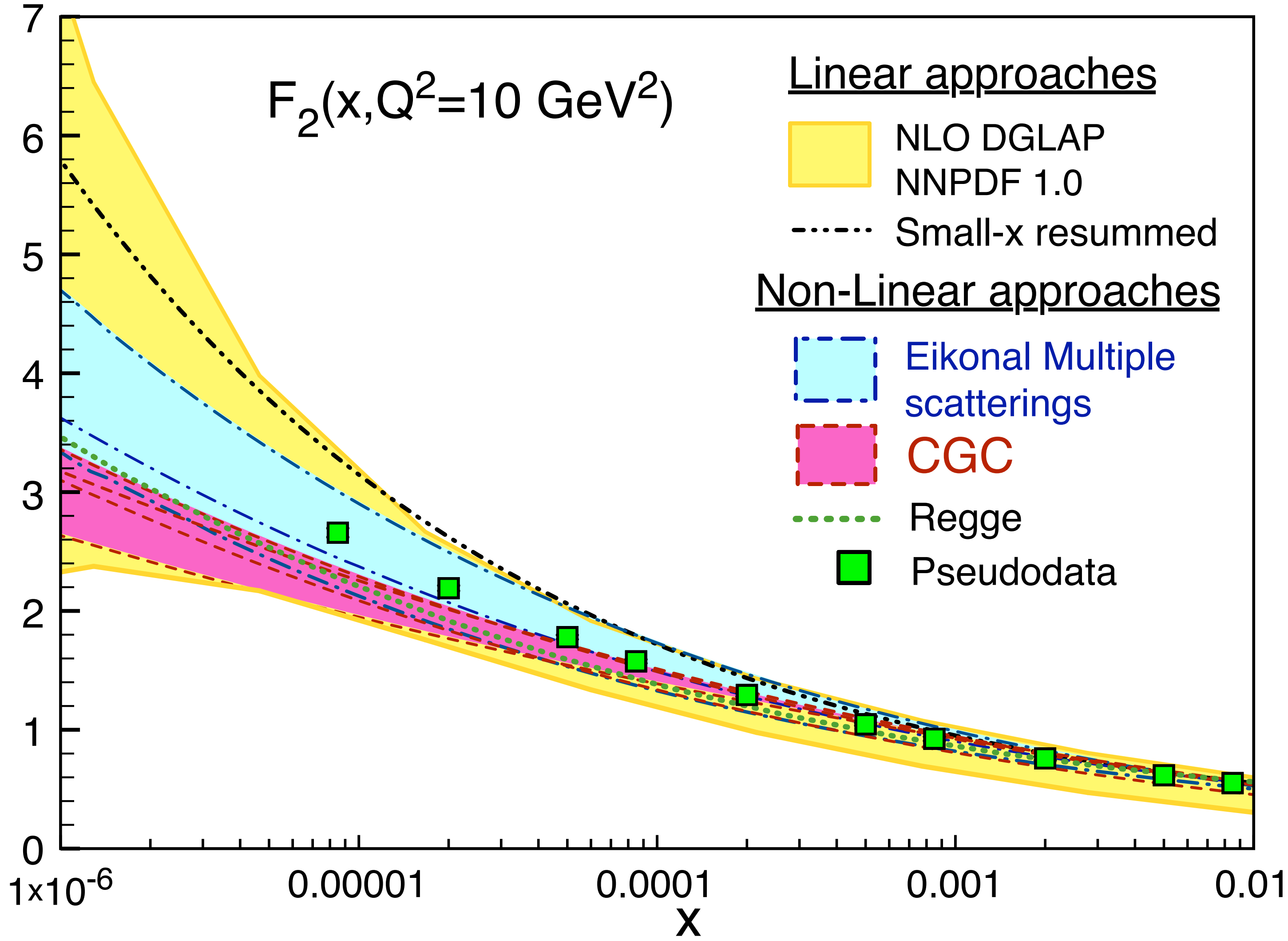

Extrapolation for FL in the LHeC kinematic regime:

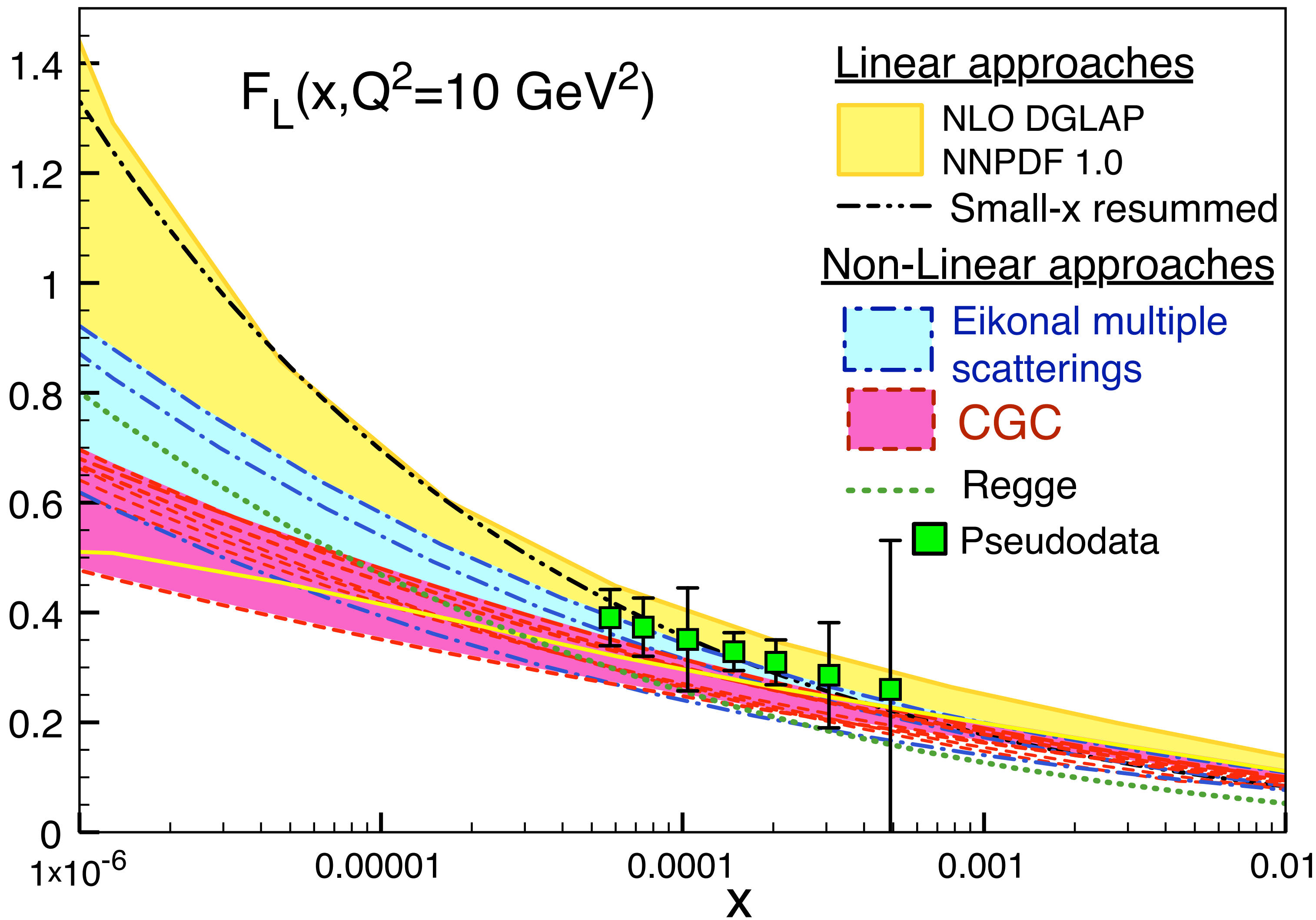

⇒ Could DGLAP also fit "CGC data"?

DGLAP (NNPDF fit) can fit pseudo-data for F2 at small-x generated by BK with running coupling (AAMS):

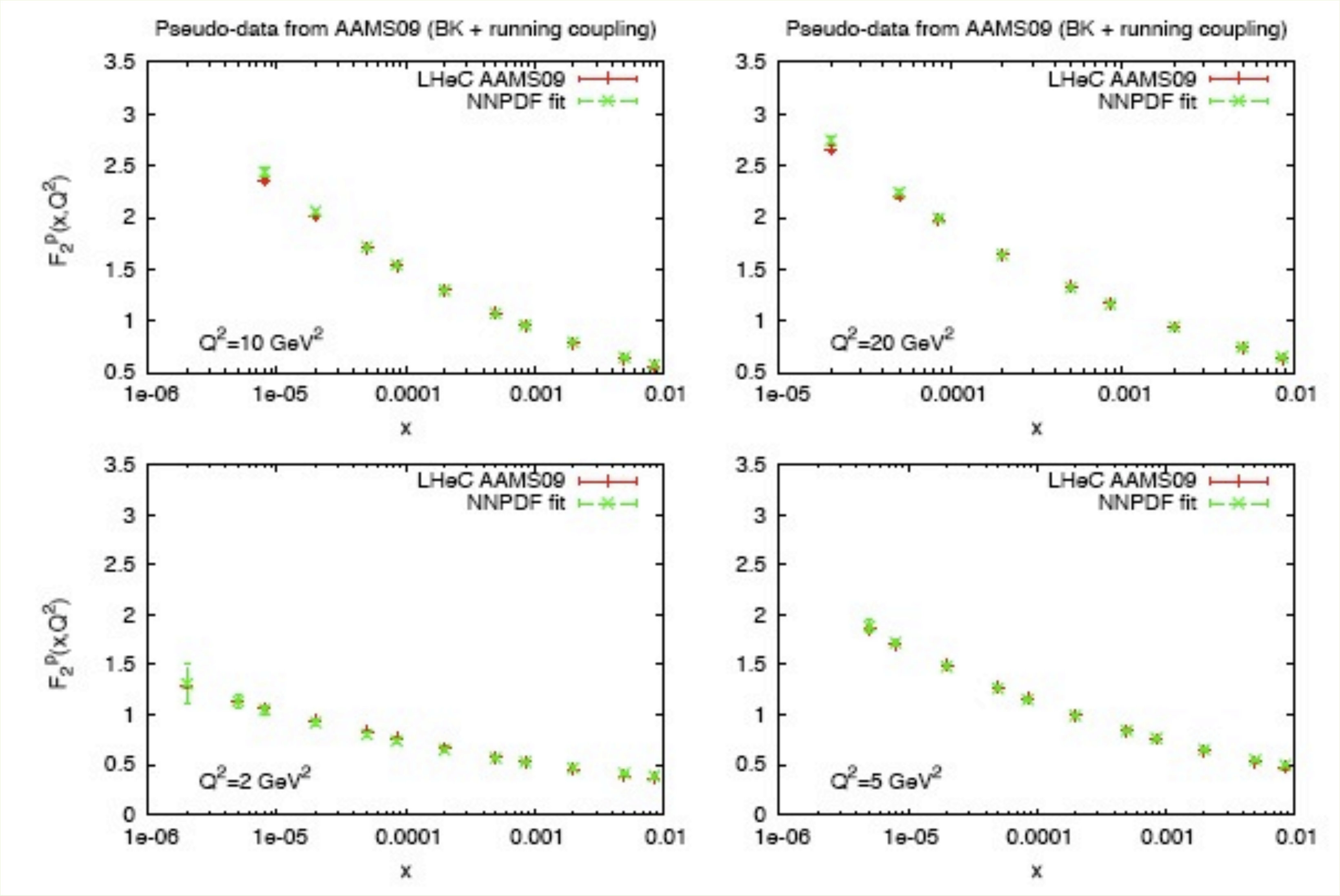

⇒ Could DGLAP also fit "CGC data"?

DGLAP (NNPDF fit) fails to fit pseudo-data for F2+FL at small-x generated by BK with running coupling (AAMS):

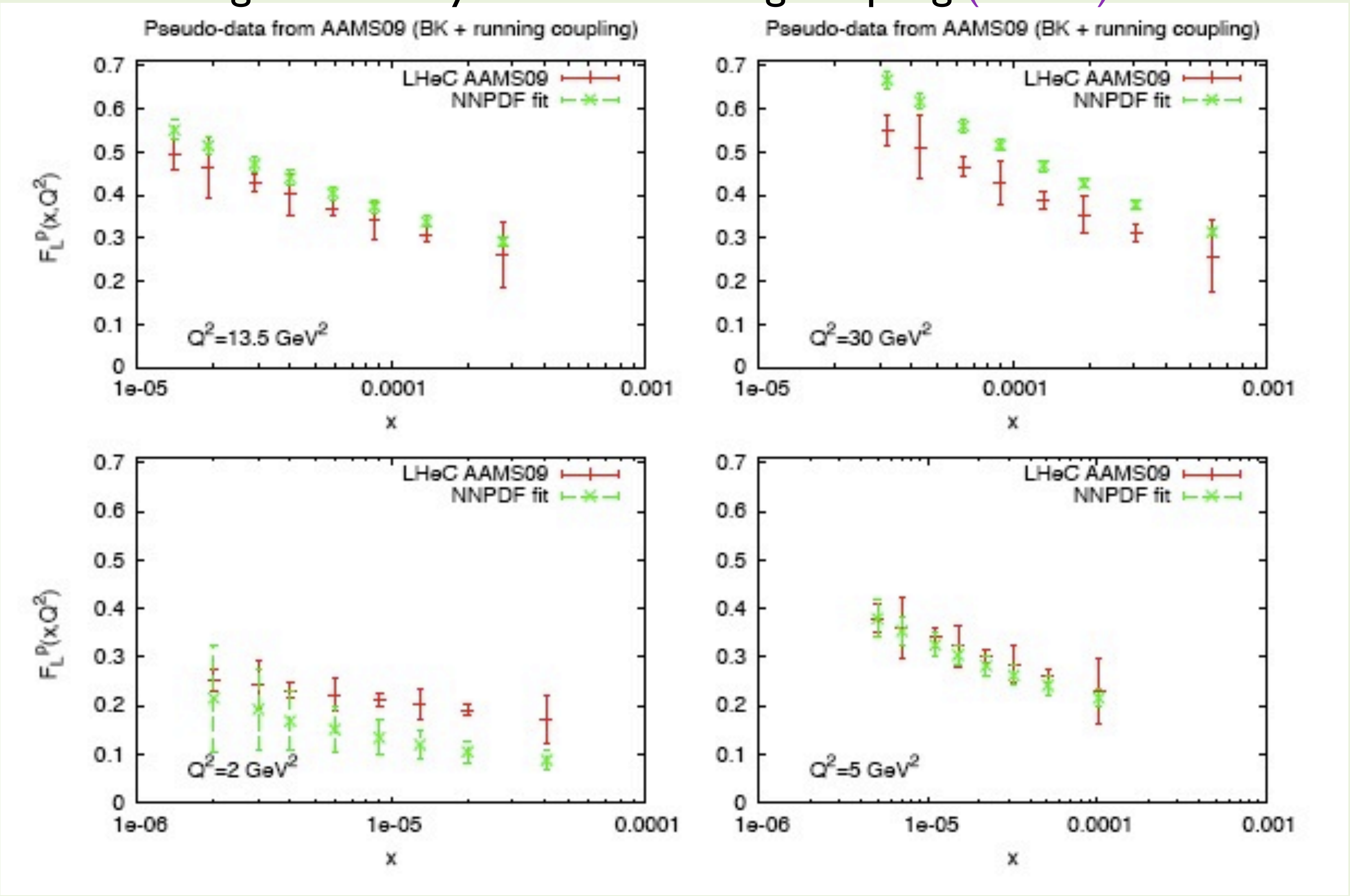

The divergence between linear DGLAP analyses and non-linear small-x dynamics is visible in FL already for $x{\sim}10^{-4}$

Conclusions:

• Little spread in LHeC extrapolations for FL and F2 from different dipole models including saturation effects: Clear theoretical reference.

• Extrapolation of DGLAP sets to small-x yields large uncertainty bands

• The BK equation (including all recently calculated corrections) provides a solid, pQCD based tool for evolution towards small-x

• At the level of inclusive observables, FL is a more promising observable than F2 for the identification of gluon recombination effects in QCD evolution

⇒ DGLAP-based models: Saturation results from eikonalization of two-gluon exchange: BGBK (Bartels-Golec-Biernat-Kowalski); IPSat (Kowalski-Teaney):

$$\frac{d\sigma^{dip}}{d^2b} = 1 - \exp\left[-\frac{\pi^2}{2\,N_c}\, r^2\, xg(x,\mu^2)T_p(b)\right]$$

$$\mu^2 = \frac{C}{r^2} + \mu_0^2$$

- The gluon distribution is fitted to data using the initial parametrization:

$$xg(x, Q_0^2 = 1\,GeV^2) = A_g\, x^{-\lambda_g}\,(1-x)^{5.6}$$

- The gluon distribution is poorly constrained by data. Good fits for

$$-0.41 < \lambda_{glue} < 0.3$$

⇓

- Large uncertainties when extrapolating towards small-x. However, very good description of HERA exclusive and diffractive data (IPSat)

Complete in $\alpha_s N_f$ Evolution JLA-Kovchegov PRD75 125021 (07).

$$\frac{\partial S}{\partial Y} = \mathcal{R}\left[S\right] - \mathcal{S}\left[S\right]$$

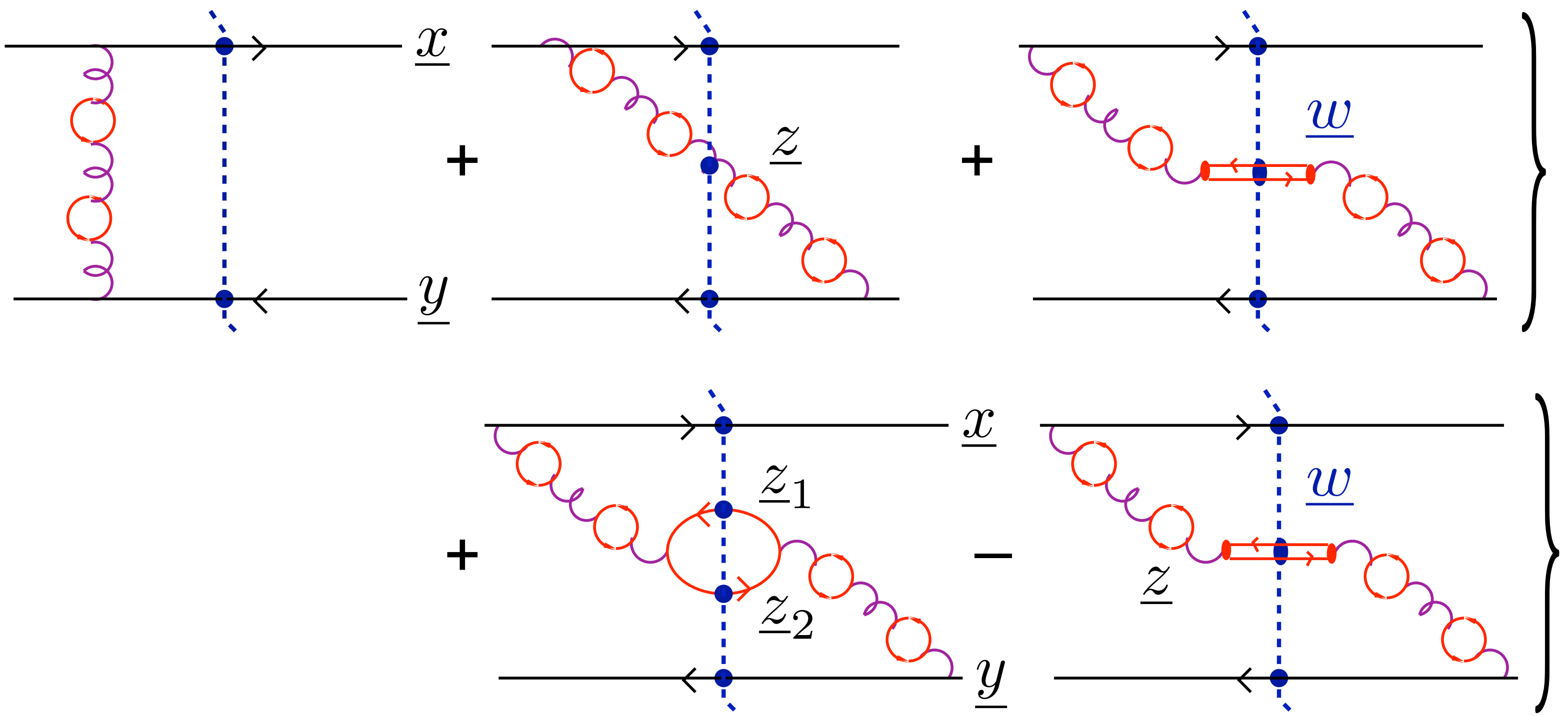

$\mathcal{R}[S]$

UV-divergent

Contributes to the running of the coupling

$\mathcal{S}[S]$

UV finite.

$\Rightarrow$ ***Running*** term: $\mathcal{R}\left[S\right] = \int d^2 z\, \tilde{K}(\underline{r}, \underline{r}_1, \underline{r}_2)\, \left[S(\underline{x}, \underline{z}) S(\underline{z}, \underline{y}) - S(\underline{x}, \underline{y})\right]$

$\Rightarrow$ ***Subtraction*** term: $\mathcal{S}\left[S\right] = \int d^2 z_1 d^2 z_2\, K_{sub}(\underline{x}, \underline{y}, \underline{z}_1, \underline{z}_2)\, \left[S(\underline{x}, \underline{w}) S(\underline{w}, \underline{y}) - S(\underline{x}, \underline{z}_1) S(\underline{z}_2, \underline{y})\right]$

Two different separation schemes: Balitsky's (BAL) and Kovchegov-Weigert's (KW)

⇒ They result in two different kernels for the running coupling kernel:

KW: $$\tilde{K}_{KW}(\underline{r}, \underline{r}_1, \underline{r}_2) = \frac{N_c}{2\pi^2}\left[\frac{\alpha_s(r_1^2)}{r_1^2} - 2\frac{\alpha_s(r_1^2)\alpha_s(r_2^2)}{\alpha_s(R^2)} + \frac{\alpha_s(r_2^2)}{r_2^2}\right]$$

BAL: $$\tilde{K}_{Bal}(\underline{r}, \underline{r}_1, \underline{r}_2) = \frac{N_c\, \alpha_s(r^2)}{2\pi^2}\left[\frac{r^2}{r_1^2\, r_2^2} + \frac{1}{r_1^2}\left(\frac{\alpha_s(r_1^2)}{\alpha_s(r_2^2)} - 1\right) + \frac{1}{r_2^2}\left(\frac{\alpha_s(r_2^2)}{\alpha_s(r_1^2)} - 1\right)\right]$$

⇒ In both cases, running coupling comes in a "triumvirate"

⇒ Balitsky's separation scheme minimizes the role of the subtraction term.

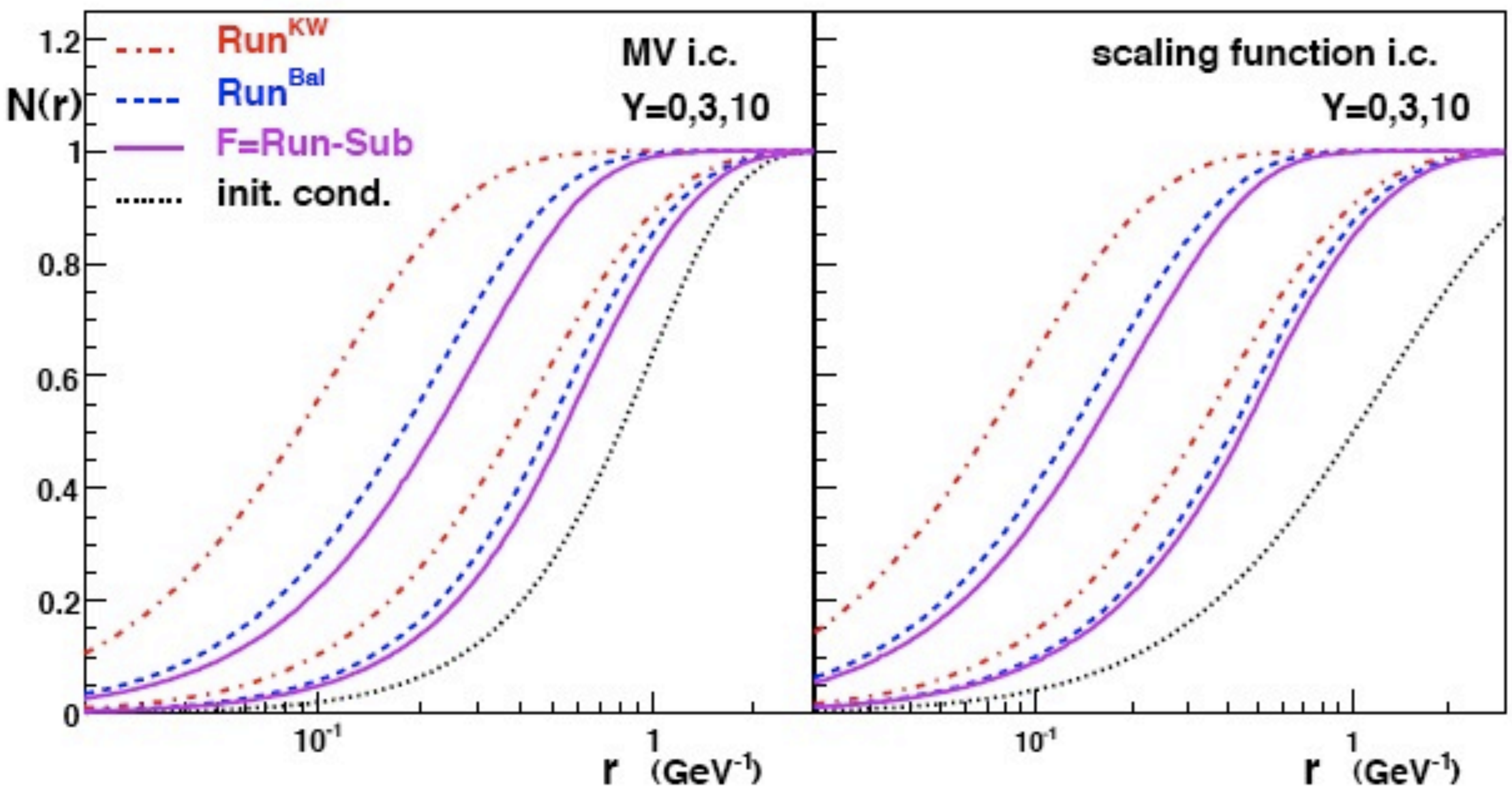

JLA-Kovchegov PRD75 125021 (07).

Fixed vs Running

⇒ The running of the coupling reduces the speed of the evolution down to values compatible with experimental data (JLA PRL 99 262301 (07)):

$$\frac{\partial S}{\partial Y} = \mathcal{R}\,[S] - \mathcal{S}\,[S]$$

$$\lambda = \frac{d \ln Q_s^2(Y)}{dY}$$

LL evolution:

$$\lambda^{LL} \approx 4.8\,\alpha_s$$

DIS data:

$$\lambda^{DIS} \approx 0.288$$

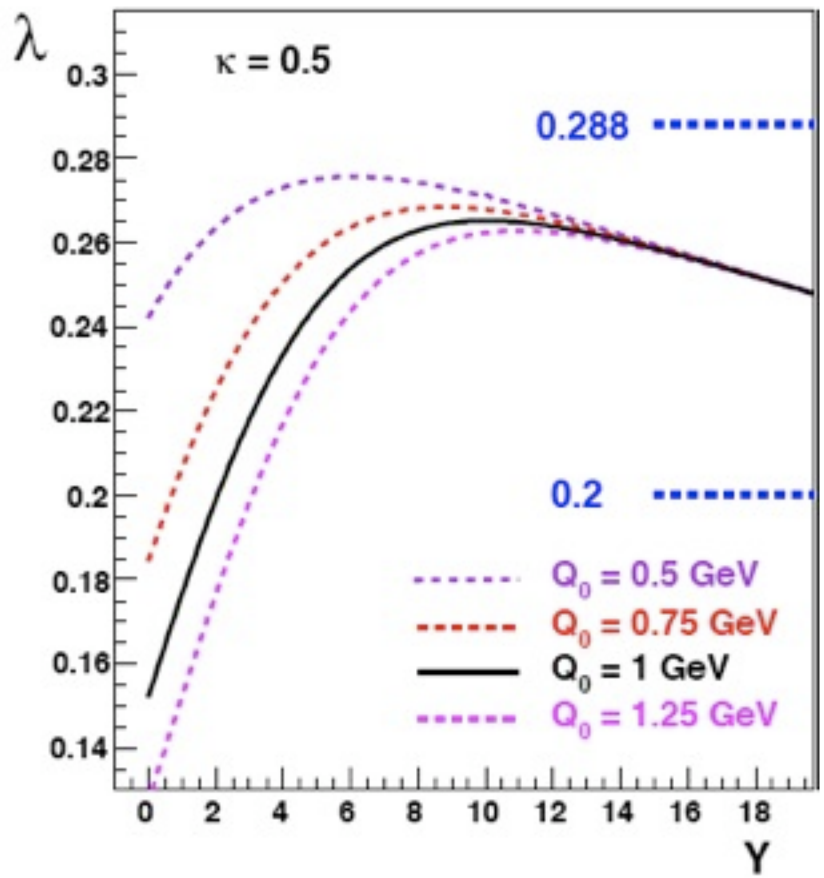

Fixed vs Running

⇒ The running of the coupling reduces the speed of the evolution down to values compatible with experimental data (JLA PRL 99 262301 (07)):

$$\frac{\partial S}{\partial Y} = \mathcal{R}\left[S\right] - \mathcal{S}\left[S\right]$$

$$\lambda = \frac{d\ln Q_s^2(Y)}{dY}$$

LL evolution:

$$\lambda^{LL} \approx 4.8\,\alpha_s$$

DIS data:

$$\lambda^{DIS} \approx 0.288$$

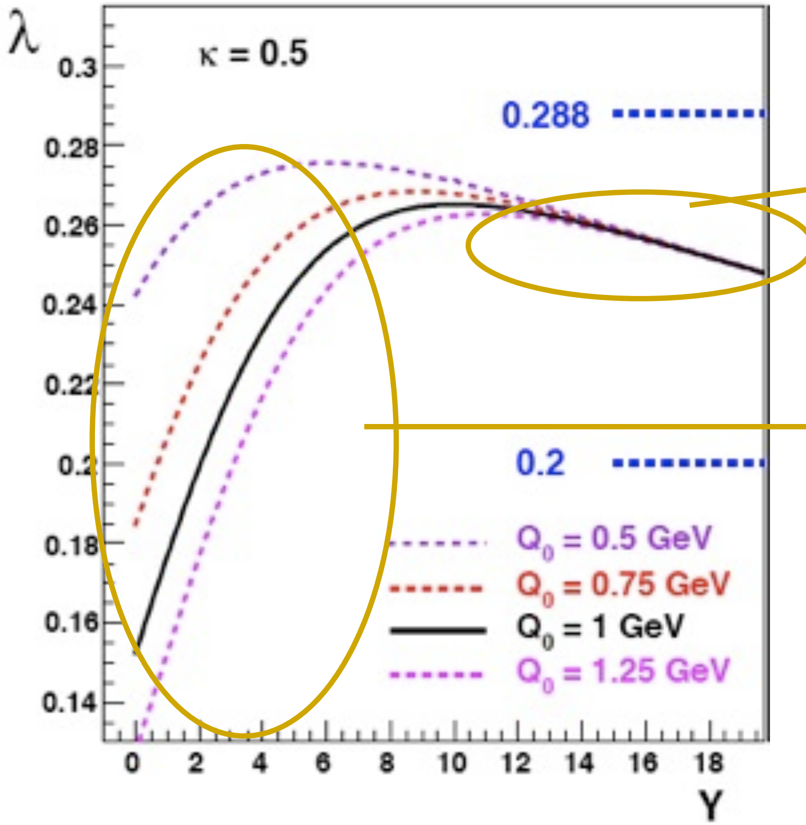

Geometric scaling

$$\lambda \sim \frac{1}{\sqrt{Y}}$$

Pre-asymptotic

⇒ The geometric scaling regime (independence on the initial conditions) is reached only at ultra-high energies

⇒ Fits to inclusive DIS structure function

$$F_2(x,Q^2) = \frac{Q^2}{4\,\pi^2\,\alpha_{em}}\,(\sigma_T + \sigma_L)$$

for x≤ 10^{-2}. 3 active flavors.

$$\sigma_{T,L}(x,Q^2) = \sigma_0 \int_0^1 dz \int d^2\mathbf{r} \left|\Psi_{T,L}^{\gamma^*\to q\bar{q}}(z,Q,r)\right|^2 \mathcal{N}(x,r)$$

⇒ x-dependence: translational invariant running coupling BK using Balitsky's prescription

$$\frac{\partial\,\mathcal{N}(x,r)}{\partial\,\ln(x_0/x)} = \int d^2r_1\,K^{Bal}(\mathbf{r},\mathbf{r_1},\mathbf{r_2})\,[\mathcal{N}(x,r_1)+\mathcal{N}(x,r_2)-\mathcal{N}(x,r)-\mathcal{N}(x,r_1)\mathcal{N}(x,r_2)]$$

$$K^{Bal}(\mathbf{r},\mathbf{r_1},\mathbf{r_2}) = \frac{N_c\,\alpha_s(r^2)}{2\,\pi^2}\left[\frac{r^2}{r_1^2\,r_2^2} + \frac{1}{r_1^2}\left(\frac{\alpha_s(r_1^2)}{\alpha_s(r_2^2)} - 1\right) + \frac{1}{r_2^2}\left(\frac{\alpha_s(r_2^2)}{\alpha_s(r_1^2)} - 1\right)\right]$$

⇒ Regularization of the coupling: We freeze to a constant, α_{fr}=0.7 in the IR:

$$\alpha_s(r^2) = \frac{12\,\pi}{(11\,N_c - 2\,N_f)\ln\left(\frac{4\,C^2}{r^2\,\Lambda_{QCD}}\right)} \quad \text{for } r < r_{fr}, \ \text{with } \alpha_s(r_{fr}^2) \equiv \alpha_{fr} = 0.7$$

$$\alpha_s(r^2) = \alpha_{fr} = 0.7 \qquad \text{for } r > r_{fr} \qquad \Lambda_{QCD} = 0.241\,\text{GeV}$$

⇒ Initial Conditions. Inspired in the GBW and MV models:

A) $$\mathcal{N}^{GBW}(r, x_0 = 10^{-2}) = 1 - \exp\left[-\left(\frac{r^2\, Q_{s0}^2}{4}\right)^{\gamma}\right]$$

B) $$\mathcal{N}^{MV}(r, x_0 = 10^{-2}) = 1 - \exp\left[-\left(\frac{r^2\, Q_{s0}^2}{4}\right)^{\gamma} \ln\left(\frac{1}{r\,\Lambda_{QCD}}\right)\right]$$

Free parameters: proton saturation scale at $x_0=10^{-2}$, Q_{s0}^2, and anomalous dimension, γ

⇒ Experimental data: ZEUS, H1 (HERA), NMC (CERN-SPS) and E665 (Fermilab) coll.

$x \leq 10^{-2}$

$$0.045 < Q^2 < 800\,\mathrm{GeV}^2$$ 847 data points

$$0.045 < Q^2 < 50\,\mathrm{GeV}^2$$ 703 data points

Fits are stable when large Q^2 data are not included in the fit

⇒ 3 (4) free parameters: Normalization, σ_0, initial saturation scale, Q_{s0}^2

IR parameter, C^2 (anomalous dimension of the i.c. γ)

Initial condition	σ_0 (mb)	Q^2_{s0} (GeV^2)	C^2	γ	χ^2/d.o.f.
GBW	31.59	0.24	5.3	1 (fixed)	916.3/844=1.086
MV	32.77	0.15	6.5	1.13	906.0/843=1.075

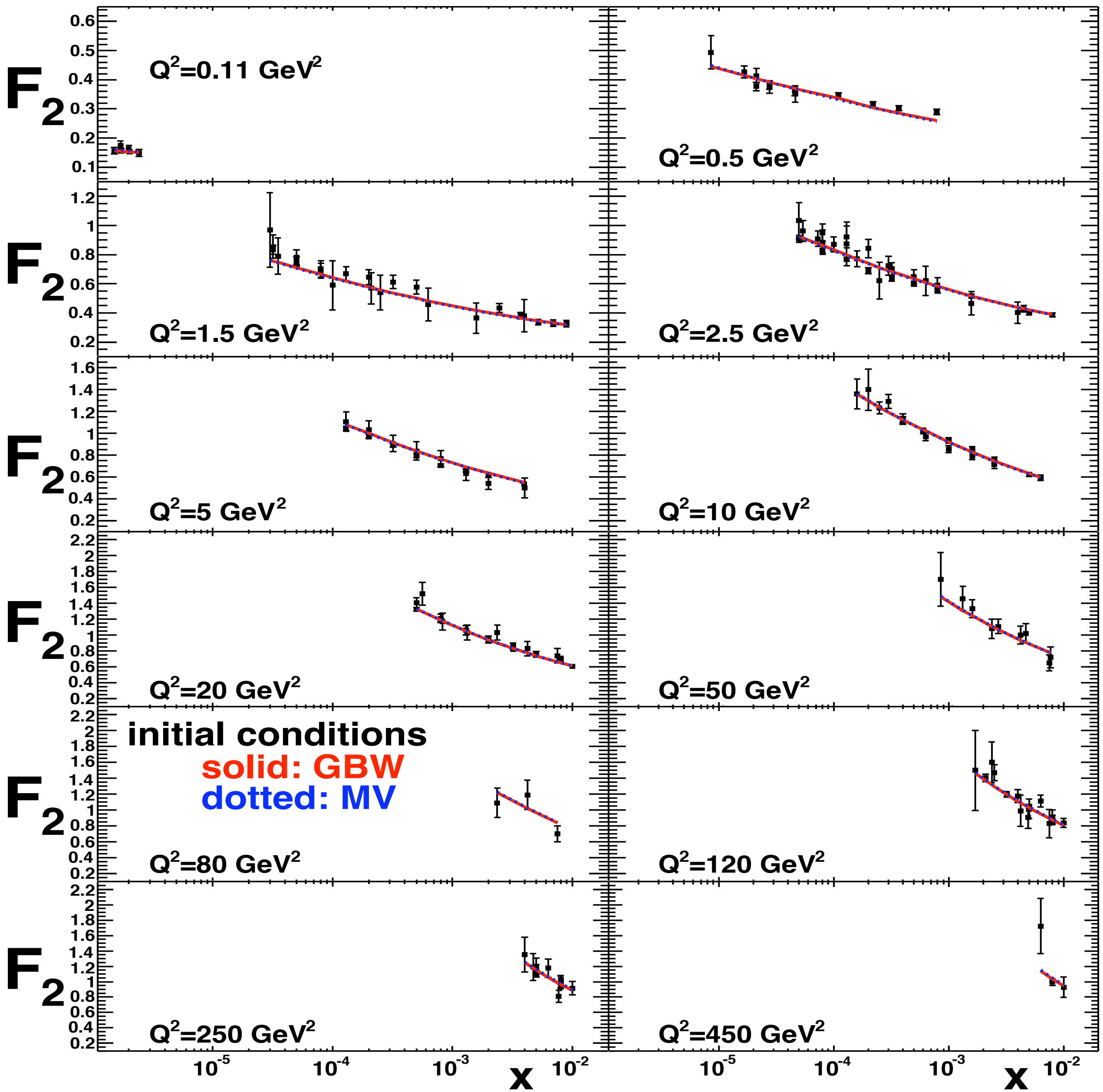

Lessons from the fits:

⇒ Fits to F2 do not constrain much the shape of the initial condition

unintegrated gluon distribution

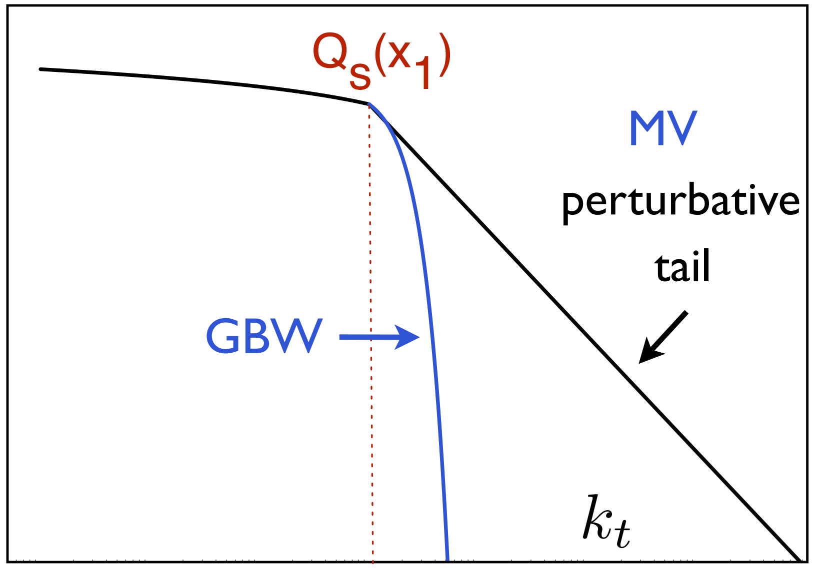

⇒ In our set up, it is impossible to fit F2 data using linear BFKL evolution:

$$\frac{\partial \mathcal{N}(x,r)}{\partial \ln(x_0/x)} = \int d^2r_1\, K^{Bal}(\mathbf{r},\mathbf{r_1},\mathbf{r_2})\,[\mathcal{N}(x,r_1)+\mathcal{N}(x,r_2)-\mathcal{N}(x,r)-\cancel{\mathcal{N}(x,r_1)\mathcal{N}(x,r_2)}]$$

⇒ Fits are stable after removing the higher Q^2 data (> 50 GeV^2)

⇒ Fits are little sensitive to the prescription followed to regularize the coupling in the IR

⇒ Good description of the longitudinal structure function:

$$F_L(x,Q^2) = \frac{Q^2}{4\,\pi^2\,\alpha_{em}}\,\sigma_L$$

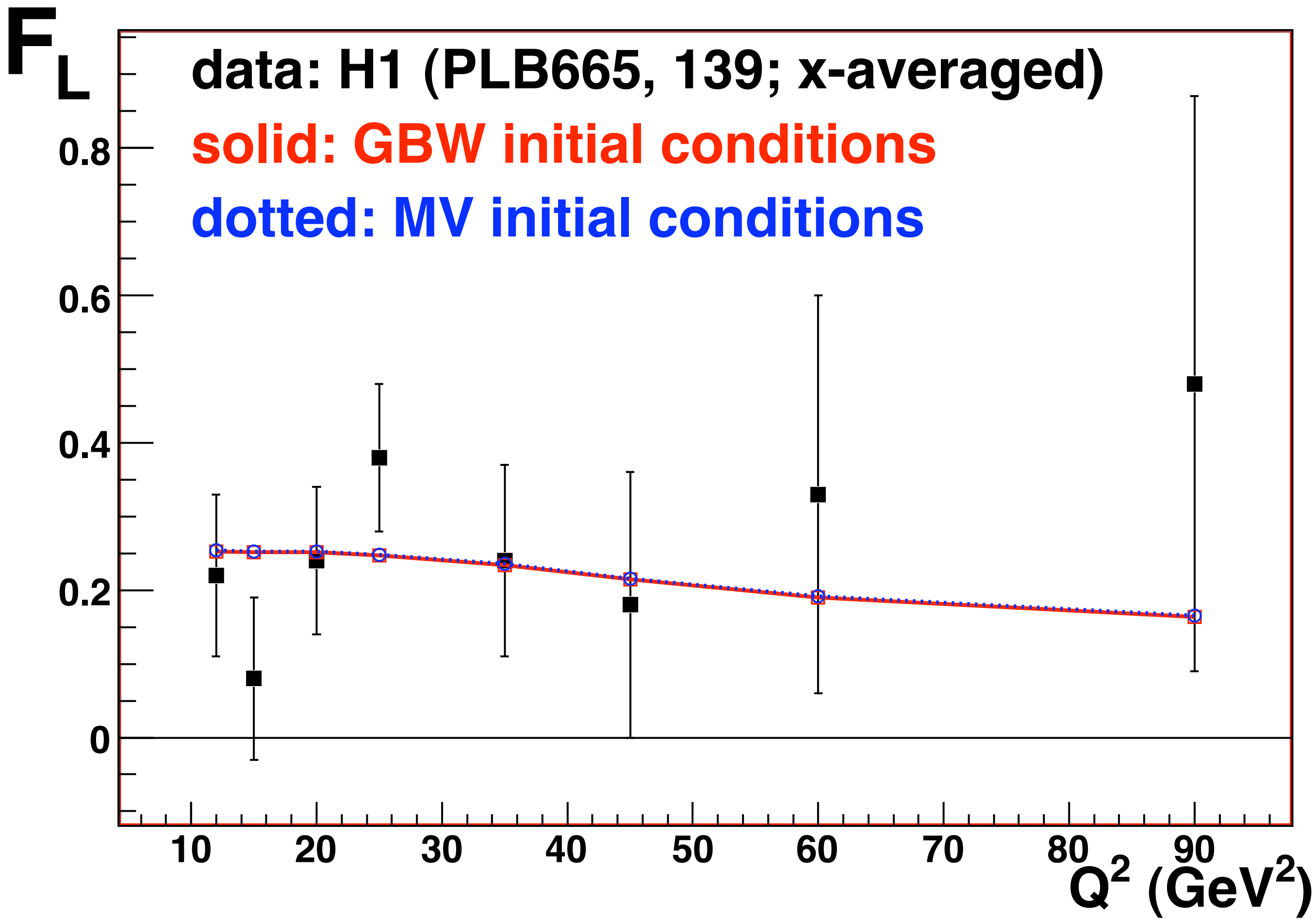

⇒ Predictions for future colliders EIC, LHeC:

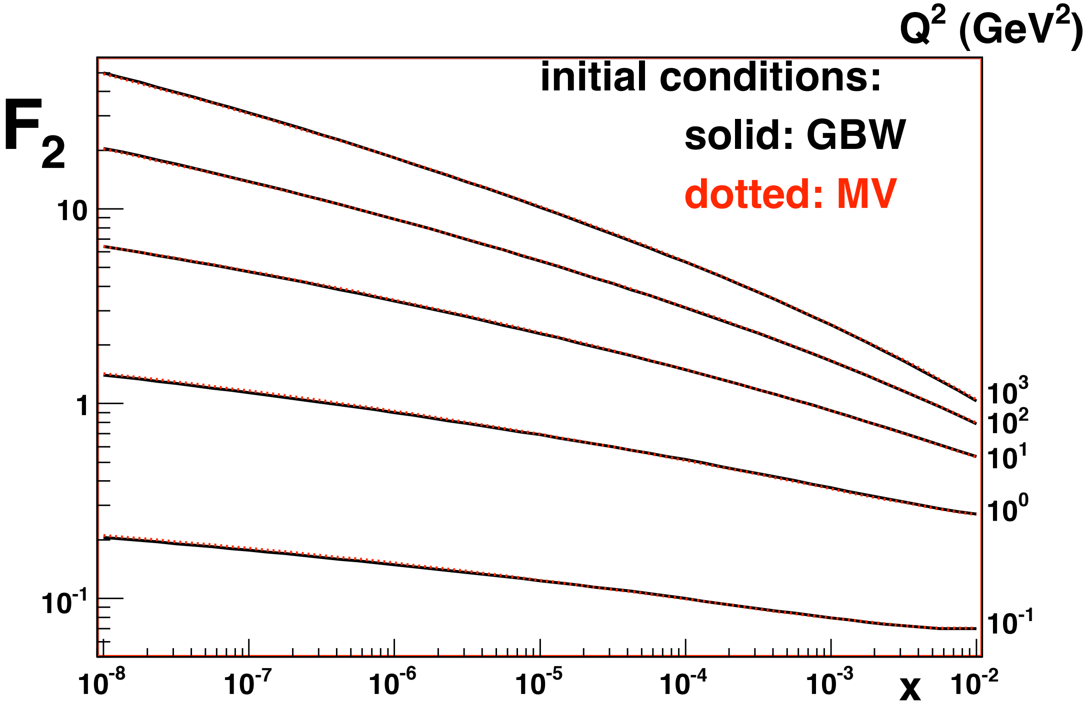

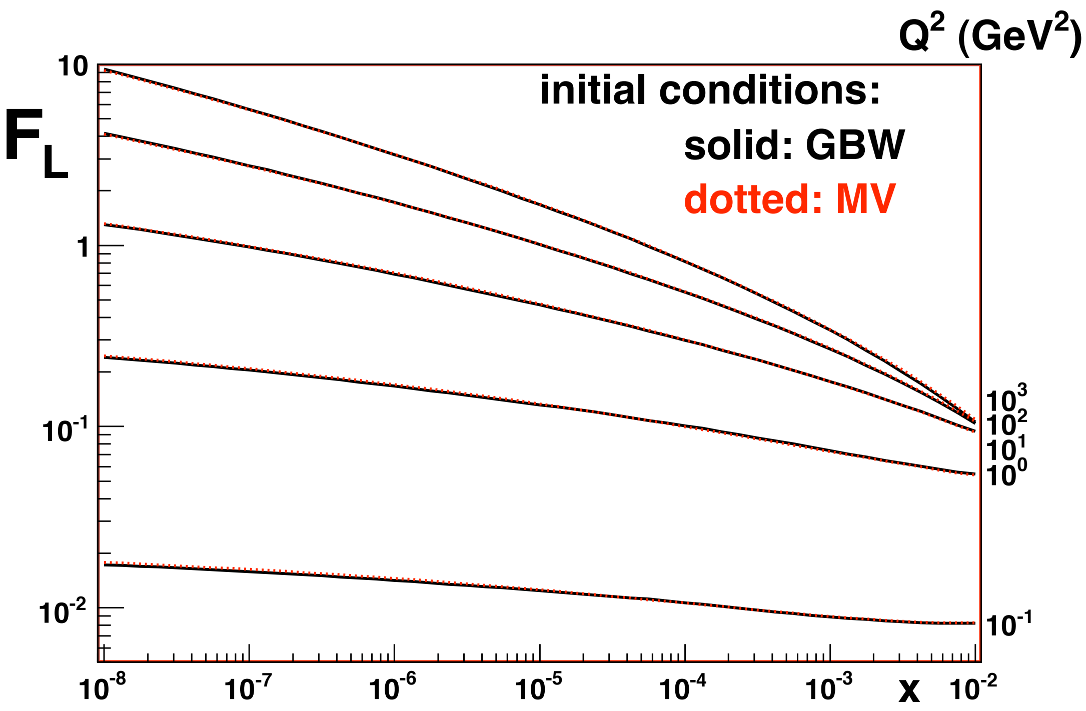

- Extrapolation to lower-x completely driven by non-linear pQCD dynamics
- Almost insensitive to i.c. Good!!!
- Saturation effects are stronger for F_L than for F_2
- F_L is a very sensitive probe of the gluon d.f. Different calculations yield pretty different predictions in the low-x low-Q2 region

⇒ BK vs DGLAP at small-x (thanks to Juan Rojo):

DGLAP (NNPDF fit) can fit pseudodata for F2 at small-x generated by BK with running coupling:

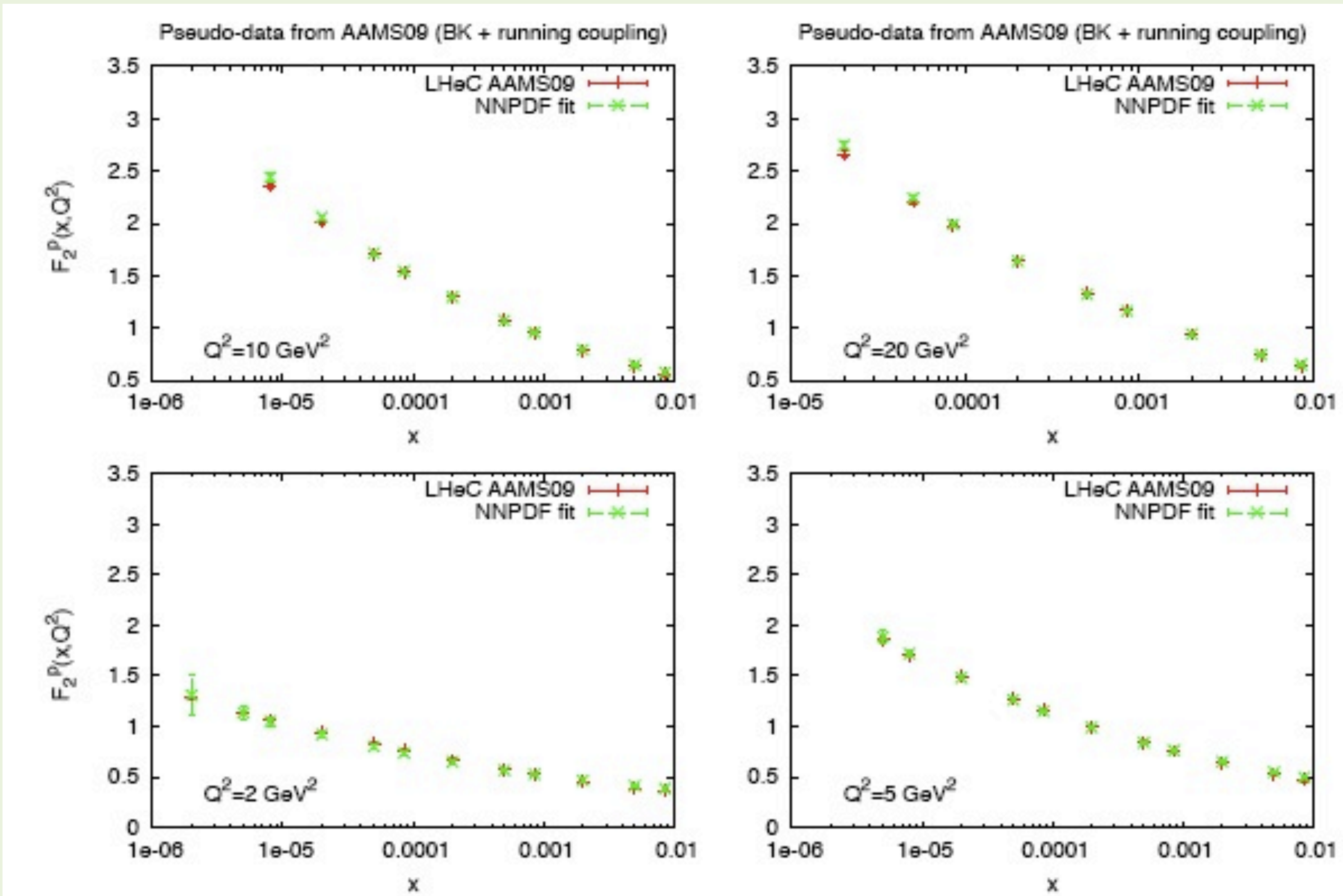

⇒ BK vs DGLAP at small-x (thanks to Juan Rojo):

However, DGALP fails to reproduce pseudodata for FL at small-x:

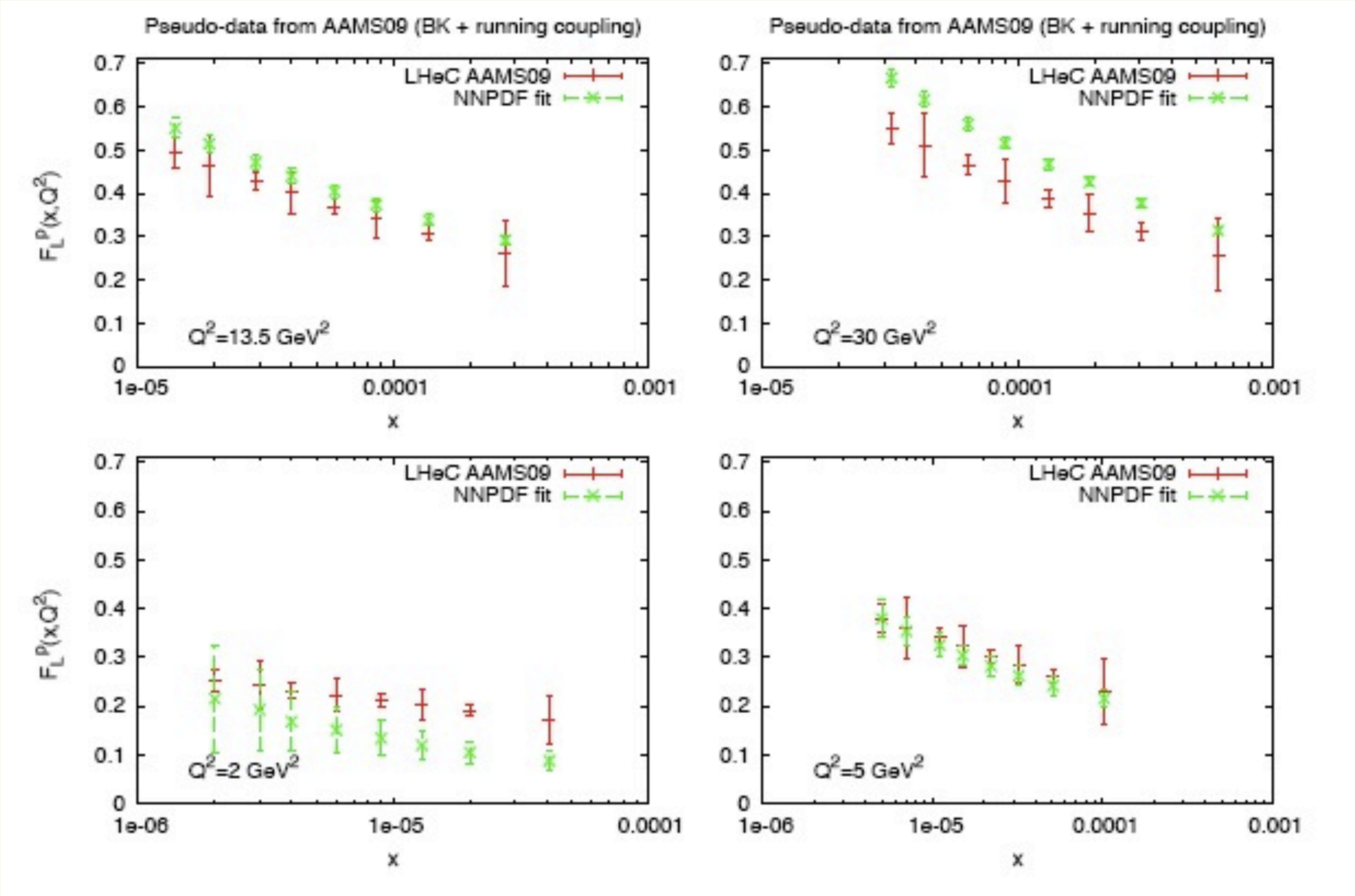

The divergence between linear DGLAP analyses and non-linear small-x dynamics is visible in FL already for $x \sim 10^{-4}$

SUMMARY

- Running coupling corrections to BK equation reconcile phenomenology and theory.
- Successful fits to inclusive DIS data using BK with running coupling.
- This is a first step in a bigger project for having non-linear pQCD controlled extrapolations to small-x (LHeC, EIC, LHC, cosmic rays) for many different observables
- Things to do next: include charm, impact parameter, nuclei...

- Parametrizations of the proton-dipole amplitude available at

http://www-fp.usc.es/phenom/software.html

BACK UP SLIDES

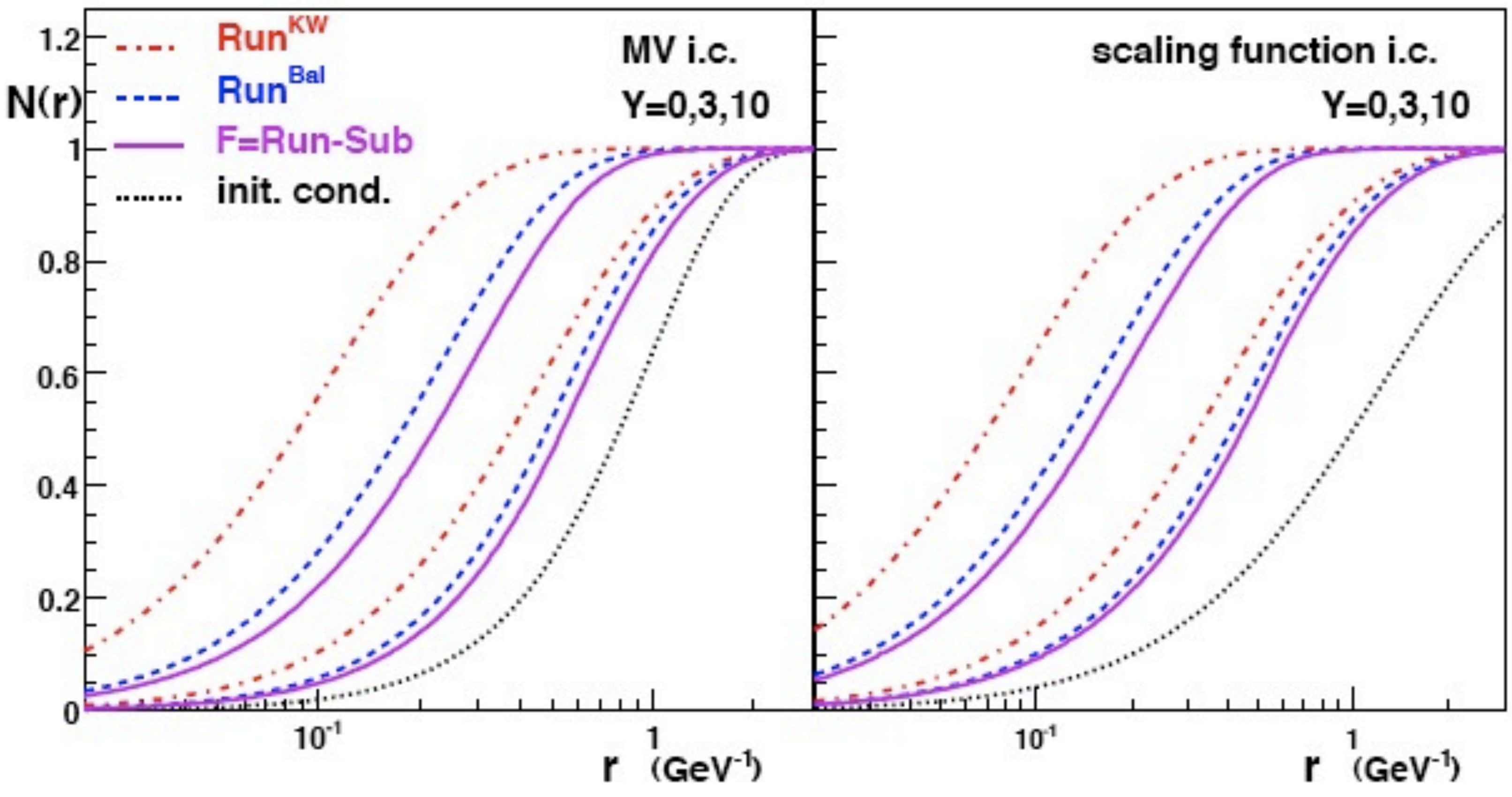

Run^KW
Run^Bal
F=Run-Sub
init. cond.
N(r)
MV i.c.
Y=0,3,10
scaling function i.c.
Y=0,3,10
1.2
1
0.8
0.6
0.4
0.2
0
10^-1
1
r (GeV^-1)

⇒ F2 is a too inclusive observable. Unable to doscriminate between very different UV behaviour of the dipole amplitude. Need to compare to more exclusive observable (inclusive particle spectra in in p-p collisions)

unintegrated gluon distribution: $$\varphi(x, k_t) = \int \frac{d^2 r}{2\,\pi\,r^2}\, \exp[i\,k_t \cdot r]\,\mathcal{N}(x, r)$$

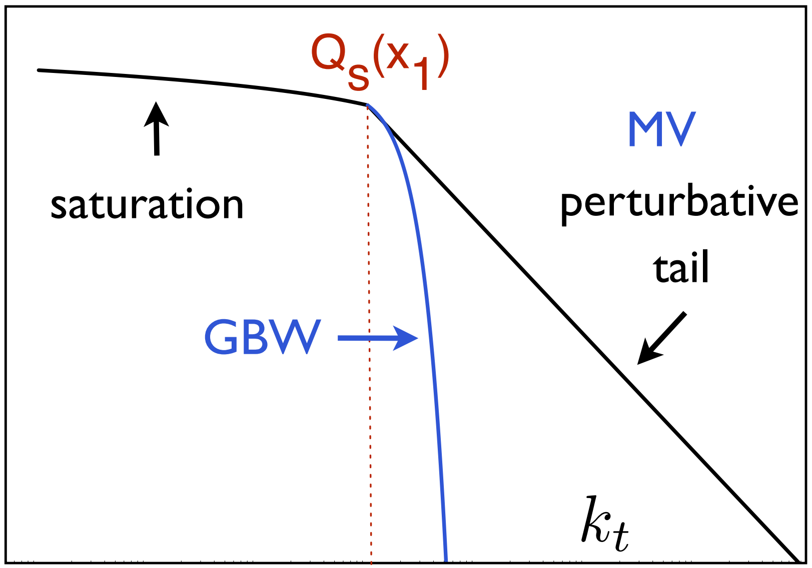

⇒ Energy and rapidity dependence of hadron multiplicities in Au-Au collsions at RHIC:

• k_t-factorization 'a la Kharzeev-Levin-Nardi'

$$\frac{dN_{AA}}{d\eta} \propto \frac{4\pi N_c}{N_c^2-1} \int^{p_m} \frac{d^2 p_t}{p_t^2} \int^{p} d^2 k_t \, \alpha_s(Q) \, \varphi_A\left(x_1; \frac{|p_t+k_t|}{2}\right) \varphi_A\left(x_2; \frac{|p_t-k_t|}{2}\right)$$

$\varphi(x,k) \Rightarrow$ Complete in αs Nf BK equation using MV i.c. $\times (1-x)^4$

$$\frac{\partial S}{\partial Y} = \mathcal{R}\left[S\right] - \mathcal{S}\left[S\right]$$

+

• 2→1 kinematics $x_{1(2)} = \frac{p_t}{\sqrt{s}} e^{\pm y}$

+

Local Hadron Parton Duality

⇒ 4 free parameters: Overall normalization, initial gold nucleus saturation scale (using MV initial condition), starting value of x for the evolution, average hadron mass

- Very good description of data at collision energies 130 and 200 GeV per nucleon:

$$Q^2_{0\,Au} \sim 0.75 \div 1.25\,\mathrm{GeV}$$

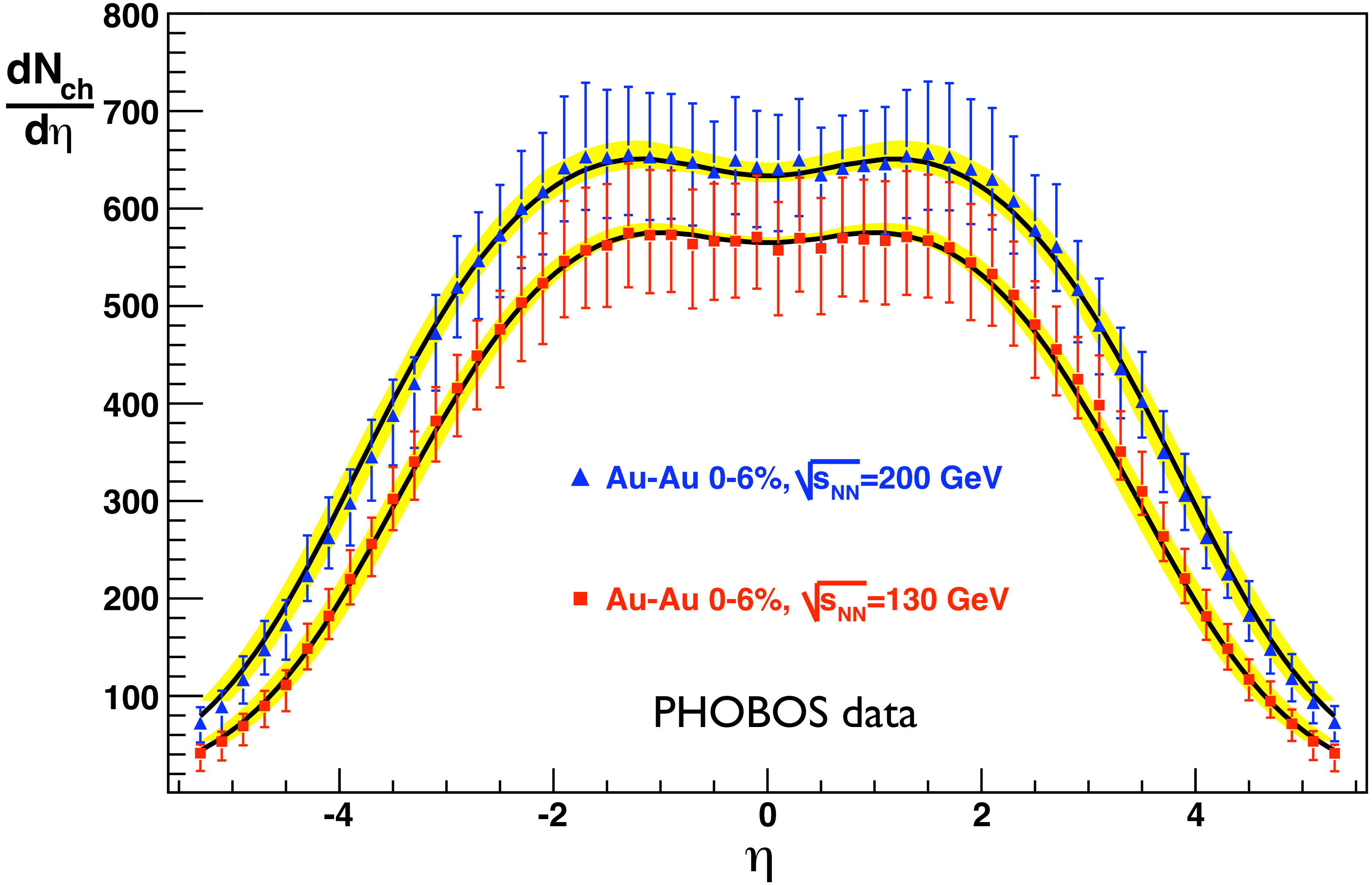

• Predictions for Pb-Pb collisions at the LHC are now completely driven by small-x evolution

$$\frac{dN_{ch}^{Pb-Pb}(\sqrt{s}=5.5\,\mathrm{TeV},\eta=0)}{d\eta} \approx 1290 \div 1480$$

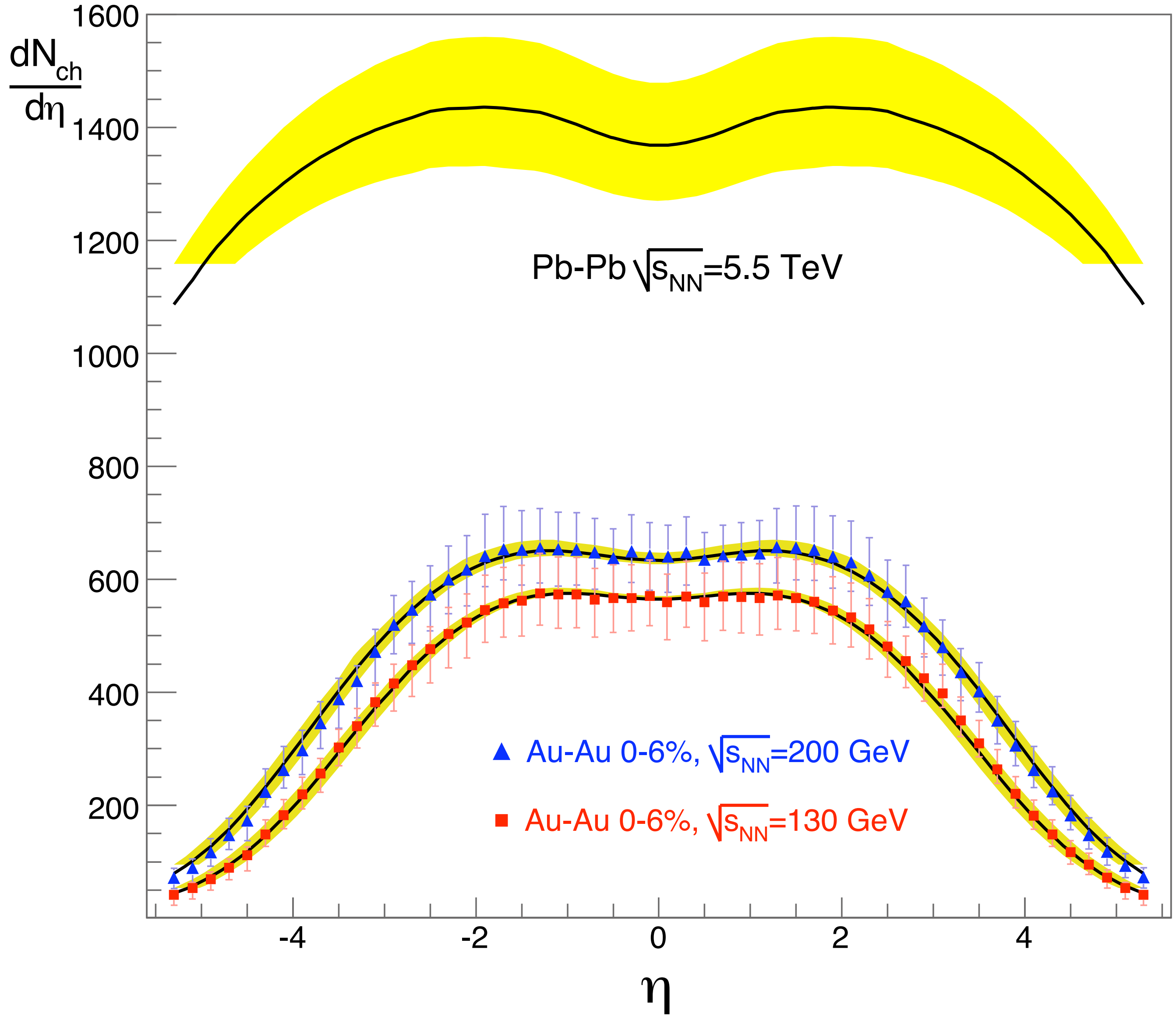

Saturation scale @ LHC

kinematics: $x \sim \frac{M}{\sqrt{s}} e^{-y}$ with $M = 1\,\mathrm{GeV}$

$$\mathcal{N}(r = 1/Q_s(x), x) = \kappa = 1 - e^{-0.25}$$

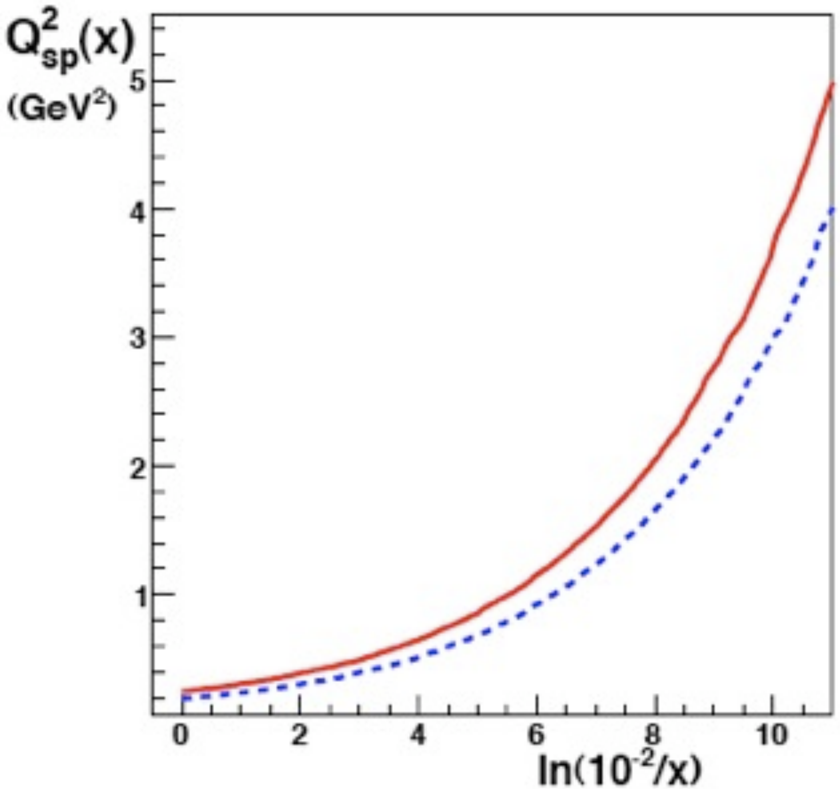

	Pb	proton
	$\sqrt{s} = 5.5\,\mathrm{TeV}$	$\sqrt{s} = 14\,\mathrm{TeV}$
y	Q_s^2 (GeV^2)	Q_s^2 (GeV^2)
0	$2 \div 2.5$	$0.65 \div 0.85$
2	$3.2 \div 3.9$	$1.2 \div 1.5$
4	$5.2 \div 7$	$2.2 \div 2.7$
6	$9 \div 12$	$4 \div 5$

$\Rightarrow$ Saturation effects may be sizable (detectable) in p-p collisions, specially at forward rapidities

- The dominant contribution to the evolution is given by the running term
- Balitsky's separation scheme minimizes the role of the subtraction term w.r.t. to KW's one

$$\frac{\partial S}{\partial Y} = \mathcal{R}\left[S\right] - \mathcal{S}\left[S\right]$$

$$\frac{\mathcal{S}\left[S\right]}{\mathcal{R}\left[S\right]}$$